

1 **Transmission network reconstruction for foot-and-mouth disease outbreaks incorporating farm-**
2 **level covariates**

3 Simon M. Firestone^{1*}, Yoko Hayama², Max S. Y. Lau³, Takehisa Yamamoto², Tatsuya Nishi⁴, Richard A.
4 Bradhurst⁵, Haydar Demirhan⁶, Mark A. Stevenson¹, Toshiyuki Tsutsui²

5

6 ¹ Melbourne Veterinary School, Faculty of Veterinary and Agricultural Sciences, The University of
7 Melbourne, Parkville, VIC 3010, Australia

8 ² Viral Disease and Epidemiology Research Division, National Institute of Animal Health, National
9 Agriculture Research Organization, Tsukuba, Ibaraki 305-0856, Japan

10 ³ Department of Biostatistics and Bioinformatics, Rollins School of Public Health, Emory University,
11 Atlanta, Georgia, United States of America

12 ⁴ Exotic Disease Research Station, National Institute of Animal Health, National Agriculture and Food
13 Research Organization, Kodaira, Tokyo, 187-0022, Japan

14 ⁵ Centre of Excellence for Biosecurity Risk Assessment, The University of Melbourne, Parkville, VIC
15 3010, Australia

16 ⁶ Mathematical Sciences Discipline, School of Science, RMIT University, Melbourne, VIC 3000,
17 Australia

18 * Corresponding author: simon.firestone@unimelb.edu.au

19

20 **Abstract**

21 Transmission network modelling to infer ‘who infected whom’ in infectious disease outbreaks is a
22 highly active area of research. Outbreaks of foot-and-mouth disease have been a key focus of
23 transmission network models that integrate genomic and epidemiological data. The aim of this study
24 was to extend Lau’s systematic Bayesian inference framework to incorporate additional parameters
25 representing predominant species and numbers of animals held on a farm.

26

27 Lau’s Bayesian Markov chain Monte Carlo algorithm was reformulated, verified and pseudo-
28 validated on simulated outbreaks populated with demographic data Japan and Australia. The
29 modified model was then implemented on genomic and epidemiological data from the 2010
30 outbreak of foot-and-mouth disease in Japan, and outputs compared to those from the SCOTTI
31 model implemented in BEAST2.

32

33 The modified model achieved improvements in overall accuracy when tested on the simulated
34 outbreaks. When implemented on the actual outbreak data from Japan, infected farms that held
35 predominantly pigs were estimated to have five times the transmissibility of infected cattle farms
36 and be 49% less susceptible. The farm-level incubation period was 1 day shorter than the latent
37 period, the timing of the seeding of the outbreak in Japan was inferred, as were key linkages
38 between clusters and features of farms involved in widespread dissemination of this outbreak. To
39 improve accessibility the modified model has been implemented as the R package ‘BORIS’ for use in
40 future outbreaks.

41

42

43 **Introduction**

44 Outbreaks of foot-and-mouth disease (FMD) in previously free countries cause severe and
45 widespread socio-economic impacts [1]. FMD-free countries therefore have stringent biosecurity
46 measures in place to prevent incursions and investigate outbreaks very thoroughly. Following a
47 review of outbreaks in non-endemic regions covering the period 1992 to 2003 [2], there have been a
48 series of costly outbreaks in previously free countries, including those in the United Kingdom in 2007
49 [3], Taiwan in 2009 [4], Japan in 2010 [5] and three independent introductions into South Korea
50 between 2010 and 2011 [6]. Many of these outbreaks are detailed in a recent review [7].

51

52 The inference of ‘who infected whom’ in infectious disease outbreaks has gained considerable
53 momentum in the wake of rapid advances in genome sequencing [8]. Accurate inference of the
54 transmission network and epidemiological parameters can aide in decision-making in the early
55 phases of an outbreak in numerous ways, including: assisting in targeting who to investigate;
56 uncovering whether unsampled (and possibly as yet undetected) sources are seeding new clusters;
57 and establishing whether or not control measures, as implemented, are effectively breaking
58 transmission. Retrospective reconstruction of outbreak networks is useful for establishing risk
59 factors for transmission and failures in biosecurity, targeting surveillance and planning for how to
60 respond most appropriately to future outbreaks. Bayesian models that combine genomic and
61 epidemiological data to infer the transmission network of outbreaks have been developed for a
62 range of emerging infectious diseases and transboundary animal diseases including highly
63 pathogenic avian influenza [9, 10], Ebola [11] and FMD [10, 12-14]. These have recently been
64 reviewed and benchmarked for application in FMD outbreaks [15]. The best-performing approaches
65 in that previous analyses were Lau’s joint Bayesian inference framework [12], the Structured
66 Coalescent Transmission Tree Inference (SCOTTI) model version 1.1.1 [14] and a modification to

67 Cottam's original frequentist approach [15, 16]. None of these models include farm-level covariates
68 other than the spatial relationship between farm locations.

69

70 In April 2010, an outbreak of FMD was detected in the Miyazaki Prefecture of Japan. This was the
71 first outbreak in the country for 10 years and prior to this outbreak vaccination had not been
72 practiced for FMD in Japan. The earliest detected infected premises (IPs) included mostly beef cattle
73 farms, with rapid spread to pig and dairy cattle farms across the extent of the Prefecture. The
74 outbreak was officially detected on 20 April 2010 based on PCR positive test results on samples from
75 cattle at a fattening farm, though non-specific clinical signs had first been detected, but not
76 diagnosed as FMD, in a cow on this farm on 9 April 2010, and even earlier, on 31 March 2010 in
77 water buffalo on a nearby farm [17]. The outbreak lasted 2.5 months, during which time 292 IPs
78 were detected and around 200,000 infected animals (cattle, pigs, water buffalos, goats and sheep)
79 were culled to contain spread. A further 87,000 animals that were vaccinated during the control
80 program were also slaughtered to expedite the resumption of international trade in livestock
81 produce. Detailed epidemiological descriptions of the outbreak, genomic analyses, risk factor
82 investigations and simulation studies have been published [5, 17-23].

83

84 The aim of the present study was to extend Lau's systematic Bayesian inference framework to
85 incorporate farm-level covariates representing the predominant species and numbers of animals
86 held on infected farms. Specific further objectives included evaluating the performance of the
87 modified model in characterising the transmission process, and estimating key epidemiological and
88 phylogenetic parameters on data from the 2010 FMD outbreak in Japan, alongside other available
89 approaches.

90

91

92 **Materials and Methods**

93 ***Model formulation and modification***

94 The model developed here is an adaptation of Lau's joint Bayesian Markov Chain Monte Carlo
95 (MCMC) inference framework [11, 12]. In Lau's original model, the total probability of individual j
96 becoming infected during time period $[t, t + dt]$ was given by:

$$r(j, t, dt) = \left\{ \alpha + \sum_{i \in \xi_j(t)} \beta k_{d_{ij}} \right\} dt + o(dt) \quad (1)$$

97 where $\xi_j(t)$ is the set of all infectious premises at time t , α is the background rate of infection, β is the
98 secondary transmission rate, $k_{d_{ij}}$ is a transmission kernel function used to represent the spatial
99 relationship between premises with $o(dt)$ representing probability of individual j being infected by
100 multiple sources of infection in the small period dt , here the power law kernel was assumed of the
101 form:

$$k_{d_{ij}} = \frac{1}{1 + d_{ij}^\kappa} \quad (2)$$

102 where d_{ij} is the Euclidean distance between the premises and κ is an inferred parameter. Other
103 options for the spatial kernel include exponential, Cauchy and Gaussian decay (not tested here).

104

105 In the present analysis, the term β in equation (1) was reformulated as β_{ij} to incorporate additional
106 terms that represent modifications to the transmissibility of each infectious farm, Inf_i , and the
107 susceptibility of each susceptible farm, $Susc_j$, such that:

108

$$\beta_{ij} = \beta \times Inf_i \times Susc_j \quad (3)$$

$$Inf_i = n_i^\nu \times (\phi_{cattle} \cdot ftype0 + \phi_{pig} \cdot ftype1 + \phi_{other} \cdot ftype2) \quad (4)$$

$$Susc_j = n_j^\tau \times (\rho_{cattle} \cdot ftype0 + \rho_{pig} \cdot ftype1 + \rho_{other} \cdot ftype2) \quad (5)$$

109

110 where n_i and n_j represent the number of animals on premises i and j , respectively, and ν and τ are
111 inferred parameters that allow for nonlinear effects of holding size [24]. We allowed three levels
112 (modulated by an indicator variable for farm type, $ftype$) for inferred parameters representing the
113 effect of the predominant species on premises i and j on transmissibility, such that ϕ_{pig} and ϕ_{other}
114 represented the component of instantaneous hazard modified by the infectiousness of
115 predominantly pig and other farms (compared to a reference category of predominantly cattle
116 farms, i.e. $\phi_{cattle}=1$), respectively, and ρ_{pig} and ρ_{other} represented the susceptibility of predominantly
117 pig and other farms (compared to a reference category of predominantly cattle farms, $\rho_{cattle}=1$),
118 respectively. This accounts for a well described biological feature of transmission whereby the
119 minimum infectious doses by inhalation for cattle, sheep and goats are much lower than those of
120 pigs, whereas infectious pigs excrete considerably more virus than these ruminant species [25] and is
121 similar in underlying structure to one of the key simulation models implemented on data from the
122 2001 FMD outbreak in the United Kingdom [24, 26]. The parameter β was retained for scaling
123 purposes. A further modification to the model was also tested, where the infectivity and
124 susceptibility terms were normalised by the population mean infectivity and susceptibility,
125 respectively.

126

127 **Model verification and pseudo-validation**

128 The modified model was verified on three FMD outbreak datasets simulated following a previously
129 described approach [27] based on Sellke thresholds [28]. These ‘model verification’ simulation runs
130 (designated J1–J3) were parameterised with the same underlying population structure as areas of

131 Miyazaki Prefecture in Japan from 2010, with differing numbers of susceptible farms and different
132 plausible transmission and genomic parameters.

133

134 The modified model was then pseudo-validated by testing on three previously described FMD
135 outbreak datasets simulated in the Australian Animal Disease Simulation (AADIS) model [29], a
136 completely different modelling framework. Corresponding phylogenetic trees nested within the
137 known transmission networks were simulated with VirusTreeSimulator
138 (<https://github.com/PangeaHIV/VirusTreeSimulator>; last accessed 31 October, 2017) and SeqGen
139 version 1.3.3 [30]. These simulated Australian FMD outbreak datasets were designated A1–A3. All
140 simulated datasets are provided in supplementary materials (S1) along with detailed descriptions of
141 their parameterisation.

142

143 ***Case study: 2010 outbreak of FMD in Miyazaki Prefecture, Japan***

144 The 2010 Miyazaki FMD outbreak datasets analysed were provided by the National Institute of
145 Animal Health and comprised premises-level covariate data on 292 infected premises and 104 L-
146 fragment consensus nucleotide sequences of virus isolates from animals on these farms, prepared as
147 previously described [5, 18, 20, 21]. Sequences were tested for recombination using RDP4 [31] and
148 for the best fitting DNA substitution model using MEGA version 7.0 [32], as assessed based on the
149 lowest Bayesian Information Criterion.

150

151 ***Model implementation***

152 The modified joint Bayesian MCMC inference of the transmission tree was implemented on a
153 parallel computing cluster with 4 chains of 1 million iterations, the first 20% of each discarded as
154 burn-in and the remainder thinned by 1000 based on assessment of convergence and

155 autocorrelation, with Gelman and Rubin's shrink factor [33], visually and by calculation of
156 autocorrelation and effective sample size using Tracer [34]. All unobserved parameters (Table 1)
157 were given uninformative flat priors and imputed as described previously [12]. The MCMC was
158 initialised with a transmission tree with initial sources selected randomly from amongst those
159 estimated to hold infectious animals at the estimated time of exposure of each IP. If there were no
160 potential sources at the estimated time of exposure of an IP the proposed source for this IP was
161 initialised with a value to represent seeding from a non-observed IP. The initiating single universal
162 master sequence was assumed to be the consensus sequence of all available genomic data.

163

164 ***Comparative analyses***

165 The 2010 Miyazaki FMD outbreak dataset was also analysed by preparing temporal transmission
166 windows [16] and inferring the transmission network and phylogenetic parameters with the SCOTTI
167 model version 1.1.1 [14], implemented in BEAST version 2.4.7 [35]. The HKY substitution model [36]
168 was assumed with 2 independent chains of 10 million MCMC iterations, each with 20% discarded as
169 burn-in and thinned by 20000 based on assessment of convergence and autocorrelation. In this
170 coalescent model with migration, each IP was modelled as a 'host', each with a distinct diverse
171 pathogen population undergoing genetic evolution. Transmissions between hosts were modelled as
172 'migration' events and the maximum number of hosts was set to 10 times the number of sequences
173 available to allow for unobserved IPs, observed IPs for which genomic data was missing and seeding
174 from external clusters. All unobserved parameters were given uninformative flat priors and the
175 following were inferred: the mutation rate, the ratio of transitions to transversions, the rate of
176 transmission between hosts, the total number of hosts (including non-sampled IPs), the number of
177 pathogen lineages per host and the tree height (from which the delay between origin and detection
178 of the outbreak could be estimated).

179

180 The code for implementing the modified Lau model has been incorporated into a freely available R
181 package named Bayesian Outbreak Reconstruction, Inference and Simulation (BORIS) [37]. The
182 descriptive analyses of all model outputs was undertaken in the R statistical package version 3.4.3
183 [38], using the libraries epiR v0.9-93 [39], statnet v2016.9 [40], coda v0.19-1 [41] and ggplot2 [42]. In
184 all comparisons, model accuracy in inferring the transmission network was considered as the
185 proportion of infected premises for which the true source was the proposed source with the highest
186 posterior probability density [15]. The effect of features of the inferred transmission network on the
187 reproductive number was inferred as previously described [43].

188

189 **Results**

190 ***Model verification and pseudo-validation***

191 The modified version of the model demonstrated improved performance in each of the simulated
192 model runs (Figure 1 and supplementary materials, S2). Overall accuracy improved by 6.2% in
193 verification runs J1–J3 (range: 5.4–6.9%) and by 4.7% in pseudo-validation runs A1–A3 (range: 2.3–
194 7.8%). Accuracy improvements occurred over the full range of model support values. Posterior
195 probability density (model support) for proposed sources was higher for outputs from the modified
196 versus the original model for all verification runs (Wilcoxon signed-rank p-values all <0.001) and
197 comparable for pseudo-validation runs; higher support has previously been associated with higher
198 accuracy. The performance of the modified-normalised version was very similar to the modified
199 version without normalisation, with the non-normalised version demonstrating typically 1–2% better
200 accuracy.

201

202 Posterior distributions of the inferred epidemiological and phylogenetic parameters are presented in
203 Supplementary Materials S3 by model run, compared to the known values. In validation runs, the
204 models were highly accurate and comparable in their inferences of α , the mutation rate and

205 transition-to-transversion ratio, farm-level latent and infectious periods, the spatial kernel shape
206 parameter (κ), and the farm-level transmissibility (ϕ) and susceptibility (ρ) weighting parameters,
207 and indices for the effects of number of animals per farm (ν and τ). In runs J1 and J2, the models
208 were highly accurate in their inference of the secondary transmission rate (β). In run J3, which had
209 an extremely low value of β all of the models overestimated the true value of 6×10^{-4} . The modified
210 model had the least discrepancy, with its highest probability density region (HPD) ranging from 2 to
211 3 times the true value, the inferred values for the original and modified-normalised models were out
212 by >200-fold. In pseudo-verification runs, the models were highly accurate and comparable in their
213 inferences of the transition-to-transversion ratio, however all three models underestimated the
214 mutation rate by between 41% and 49%. The rest of the inferred parameters are not directly
215 analogous to those used in the simulation framework for pseudo-validation, so could not be directly
216 compared to known values.

217

218 ***Case study: 2010 outbreak of FMD in Miyazaki Prefecture, Japan***

219 Each of the 104 sequences were 7667 nucleotides in length, no recombination was detected. The
220 best-fitting nucleotide substitution model was the Tamura-Nei (TN93) model with non-uniformity of
221 the evolutionary rate among sites represented using a discretised Gamma distribution with five
222 categories, an estimated shape parameter of 0.13, assuming that none of the sites were
223 evolutionarily invariable and a transition to transversion ratio of 9.08 (see supplementary materials,
224 S4 for further detailed results).

225

226 The transmission network inferred using the modified Lau MCMC algorithm is presented in arbitrary
227 space in Figure 2. Posterior estimates of the key epidemiological and phylogenetic parameters from
228 the modified version of the Lau model are presented in Table 2. Networks for the original and
229 modified-normalised model formulations are provided as Supplementary Materials (S5) highlighting

230 differences to the presented network. The root of the inferred transmission tree was inferred with
231 very high model support. Transmission from an external source was inferred to have most likely
232 occurred 31 days prior to the outbreak being detected (i.e., on 19 March 2010; 95% HPD: 8 and 25
233 March 2010). At the point of outbreak detection (on 20 April 2010) it was inferred that there were
234 15 farms already infected. The median diagnostic delay (time from inferred exposure at a farm until
235 day of sampling) was estimated to be 9.7 days (range: 4.6, 32.9 days).

236

237 Of the 292 IPs, only 47 had a proposed source from Lau's modified algorithm with model support
238 >50%, of these only 18 links had model support >80%. Model support was highest for inferred
239 transmission events earlier in the outbreak (geometric mean support for events in first 4 weeks was
240 74.8%, whereas for events in the mid and latter 4-week periods of the outbreak geometric mean
241 support was 24.1% and 12.2%, respectively), likely relating to the density of genomic sampling. The
242 longest of the inferred chains of infection involved 8 transmission events, with 93% of transmission
243 chains being ≤ 5 events in length. The scale-free properties of the transmission network's out degree
244 distribution (coefficient of variability = 3.3), suggested a multiplying effect on the basic reproductive
245 number of 12.0. The geometric mean number of secondarily infected premises for IPs exposed in the
246 first 4 weeks of the outbreak was 5.9, dropping to 3.2 and 1.3 for IPs exposed in the middle and
247 latter 4-week intervals of the outbreak, respectively. This demonstrates the effectiveness of animal
248 movement controls and other measures.

249

250 Farms that kept predominantly pigs were 5.15 times more infectious than cattle farms (Table 2). The
251 eleven farms that were inferred to have led to the highest number of secondary infections were all
252 pig farms. Those farms that predominantly kept other species appeared less infectious than cattle
253 farms, however as there were only five 'other' farms the HPD for ϕ_{other} crossed the null value of 1.
254 Farms that kept predominantly pigs were 49% less susceptible than cattle farms. Those farms that

255 predominantly kept other species were 55% less susceptibility than cattle farms (noting that the HPD
256 again crossed 1, due to low numbers in this group). The number of animals on a farm had more
257 influence on farm-level susceptibility than infectivity.

258

259 The posterior estimates of the mean farm-level incubation, latent and infectious periods were 5.9,
260 6.8 and 15.2 days, respectively. Based on the shape of the inferred spatial transmission kernel
261 (Figure 3), most of the density of risk is within 15 km of an infected premises. Most parameter
262 inferences were highly comparable across model runs (modified versus original and normalised). An
263 exception was the secondary transmission rate (β) which from the modified-normalised model
264 outputs was inferred to be an order of magnitude higher than as inferred in the original and
265 modified formulation. The HPDs of most of the inferred parameters overlapped with those used in
266 the model verification runs J1–J3.

267

268 ***Comparative analyses***

269 Transmission windows estimated by Cottam’s approach, are presented for the 20 IPs with earliest
270 dates of onset in Figure 4. Based on this approach, at least ten IPs had already been exposed by the
271 time the outbreak was detected. There were only seven IPs for which the Lau modified and SCOTTI
272 models agreed on source. Amongst the 104 IPs for which genomic data were available, proposed
273 sources for 13 IPs inferred by the SCOTTI algorithm were on the transmission pathways inferred by
274 the Lau model (which included both sampled and unsampled sources).

275

276 The posterior median estimates of the substitution rate and transition to transversion ratio inferred
277 by SCOTTI were highly comparable to those inferred by Lau’s model, with overlapping HPDs that also
278 encompassed the maximum likelihood value estimated using MEGA. The SCOTTI model suggested

279 the sequence data were monophyletic (i.e., a single introduction), with only a single likely root and
280 transmission from the original external source was estimated to have occurred 39 days prior to
281 detection of the outbreak (i.e. on 12 March 2010). Onward transmission from the source occurred at
282 a rate of 3.2 new infected premises per day over the course of the outbreak, with the median
283 estimate of the number of FMD viral lineages within each farm being 19. Of those 104 IPs with
284 genomic sequence data available, only 32 had consensus support that their proposed source was
285 amongst those sampled and of these only 5 had >50% model support for their proposed ancestor
286 (detailed results provided as Supplementary Materials, S6). Based on the structured coalescent
287 transmission tree inference, there was very low likelihood that the source of infection for the first
288 farm inferred to have been infected in this outbreak was amongst those sampled (support = 2.4%),
289 whereas it was much more likely that the index farm's source was amongst those sampled (support
290 = 33.4%) and model support that the index was infected by the first farm inferred to have been
291 infected approached consensus (42.8%).

292

293 **Discussion**

294 Transmission network models that enable reconstruction of outbreaks hold considerable promise for
295 informing decision-making in future outbreak responses if they are accurate, robust, reproducible,
296 reliable and can be implemented with ease. Here, we have developed and evaluated an extended
297 version of Lau's systematic Bayesian inference framework incorporating additional parameters to
298 infer farm-level effects on transmissibility and susceptibility related to the predominant species on a
299 property and the numbers of animals kept. The modified model demonstrated improved
300 performance across a series of varied simulated outbreaks, with overall accuracy improving by
301 between 5 and 6%. These improvements may seem modest unless considered from the perspective
302 that Lau's original model was already a well-performing highly detailed inference as recently
303 demonstrated [15] and the modified model is intended to be implemented in near-real time in

304 outbreaks involving hundreds of infected farms, where each correctly inferred link may aid the
305 speed of containment and subsequently greatly reduce future outbreak impacts.

306

307 The inferred transmission network for the 2010 outbreak of FMD in Japan identified all key linkages
308 between clusters and characterised features of important farms in widespread dissemination of this
309 outbreak. Pig farms played a vital role, with most of the farms forming hubs in the transmission
310 network holding predominantly pigs. This has previously been identified as key to dissemination of
311 FMD [25, 44], however, with the inclusion of additional parameters, we were able to estimate the
312 magnitude of this effect alongside other important epidemiological and phylogenetic parameters.

313 The five-fold increase in transmissibility of pig farms compared to farms holding predominantly
314 cattle is biologically plausible and agrees with published accounts that, depending on FMD strain,
315 pigs can excrete up to 100 times more airborne virus at the peak of the viraemic phase than cattle
316 [25]. Whilst pigs may excrete more virus than ruminants, cattle on a downwind farm are more
317 susceptible to infection via inhalation. Although pig farms tend to hold more animals, they also
318 typically implement management measures specifically focussed on hygiene, biosecurity, ventilation,
319 humidity and temperature control, odour and pollution reduction that would be expected to
320 influence and often reduce the potential for disease dissemination.

321

322 The effect of numbers of animals held suggested farm size had more of an influence on farm
323 susceptibility than transmissibility, however the HPDs of the inferred parameters representing these
324 non-linear effects overlapped considerably. This modification was stimulated by the formulation of
325 previous FMD models for the 2001 outbreak in the United Kingdom [24] and despite minor
326 differences in parameterisation the estimates were all reasonably close to those fit to that prior
327 outbreak. In some of the regions previously studied in the UK 2001 outbreak, numbers of animals
328 held influenced transmissibility more than susceptibility, but the finding was not consistent. Such

329 differences likely relate to differences in the predominance of sheep versus pigs in different regions
330 and their differing influences on transmission. In their analysis, Tildesley and colleagues (2008)
331 included species-specific parameters to represent the nonlinear influence of numbers of animals
332 held. When we attempted to include such species-specific parameters in the modification to Lau's
333 approach, this led to over-parameterisation and presumed identifiability issues impacting on MCMC
334 chain mixing and convergence. We therefore settled for a single parameter for each effect, assuming
335 that species-specific effects should be well represented by the specific farm-level susceptibility and
336 transmissibility terms.

337

338 The inferred farm-level incubation period in the 2010 FMD outbreak in Japan of 2–14 days
339 corresponds very closely with previously published data [25, 45]. Interestingly, at the farm-level, the
340 median inferred incubation period was 1 day shorter than the median latent period. This finding is
341 consistent with an experimental study where the relationship between onset of infectiousness was
342 based on directly demonstrating FMD transmission to another animal [46]. In contrast, many studies
343 that have considered onset of infectiousness at the farm-level based on proxy measures (such as
344 detection of virus in blood, nasal fluid and/or oesophageal-pharyngeal fluid) [45] may have
345 underestimated the duration of the latent period [46]. Whilst individual animals have been shown to
346 excrete FMD virus 1–2 days before onset of clinical signs [47-49], this depends on dose and FMD
347 virus strain, and there is marked individual variability in the onset of early clinical signs in pigs and
348 cattle. It is important to note that the unit of interest in the present analysis is the farm and these
349 epidemiological parameters are therefore observed at the farm-level, whereas most studies of the
350 timing of onset of infectiousness and clinical signs focus on the animal-level. Also, the observed
351 epidemiological data that informed our inferences were from field observations, rather than based
352 on experimentation, and thereby include a certain level of uncertainty. Nonetheless, these
353 epidemiological parameters are very helpful for informing disease response activities (quarantine
354 periods, surveillance and contact-tracing windows), and estimates from observed outbreak such as

355 those presented here are vital for parameterising FMD simulation modelling. Similarly, the farm-
356 level infectious period is a very important parameter, seemingly intuitive but given all the factors at
357 play difficult to interpret. Often, as in the present analysis, the farm-level infectious period is cut
358 short by culling and other disease control activities. In the 2010 outbreak of FMD in Japan, targeted
359 vaccination was only implemented for 5 days at the peak of the outbreak [17], so was not
360 considered to have had a major impact on the inference of epidemiological parameters.

361

362 With data augmenting MCMC approaches, as implemented here, reconstructing such outbreaks
363 need not be completed years after the outbreaks are over. It is a primary intention of the design of
364 these models that they be implemented to inform ongoing disease responses. Indeed, these models
365 are presently being implemented in near-real time to inform the ongoing outbreak of *Mycoplasma*
366 *bovis* in New Zealand [50]. As detailed in the present analysis, these models provide statistically
367 justifiable inference of which premises were primary sources in an outbreak and the timing of
368 exposure at those farms. This can greatly inform targeting of contact-tracing windows and farmer
369 interviews to high-risk periods and help identify undetected sources of such outbreaks before
370 further clusters can be seeded. An active area of further research includes incorporating contact-
371 tracing and other animal movement data into this model. Further areas for development include
372 refining the representation of genomic evolution through the implementation of within-host
373 dynamics such as has been implemented in other transmission network models [10] and formally
374 predicting undetected infections with Reversible-Jump MCMC or related methods [51].

375

376 The original attempts at FMD outbreak transmission network modelling have largely focussed on
377 small subsets of large outbreaks [10, 12, 16, 52]. With the present modified formulation, we have
378 demonstrated inference for outbreaks involving up to 400 premises, and with typically available
379 parallel computing infrastructure it presently appears feasible to run inferences for outbreaks of

380 over 500 premises with some further efficiencies in coding. The present analysis was limited in the
381 number of simulations that could be feasibly undertaken for model verification and pseudo-
382 validation. However, we consider the additional gain in information will be modest with further
383 testing on substantially increased numbers of simulation runs. In the present analysis, all models had
384 difficulties inferring secondary transmission rates when these were very low. The best-performing
385 model was again that with the modification to incorporate farm-level effects on transmissibility and
386 susceptibility. The low value for β tested in verification run J3 was perhaps unrealistic being 100
387 times below the inferred values based on the actual outbreak data from the 2010 outbreak in Japan.
388 The mutation rate appears to be underestimated by all forms of the Lau model. This is not a major
389 concern, as the primary purpose of this model is to infer the transmission network. More purposeful
390 phylogenetic tools, such as BEAST and associated packages [35, 53], are preferable when the primary
391 aim is estimation of such phylogenetic parameters and more sophisticated models including
392 additional complexities such as within-host diversity are available. Nonetheless the mutation rates
393 inferred by the modified Lau model overlapped with those of the SCOTTI model implemented in
394 BEAST2.

395

396 The present analysis was limited in the number of simulations that could be feasibly undertaken.
397 However, we consider the additional gain in information will be modest with further testing on
398 substantially increased numbers of simulation runs. In the present analysis, all models had
399 difficulties inferring secondary transmission rates when these were very low. The best-performing
400 model was that with the modification to incorporate farm-level covariates.

401

402 There was poor agreement between the transmission networks inferred by SCOTTI and the Lau
403 modified model. Reasons for differences in transmission network inferences include different
404 underlying likelihood formulations and data requirements. Specifically, the Lau model infers

405 sequences for known IPs for which genomic data is unavailable and incorporates terms that account
406 for the spatial relationships between infected premises. For four IPs that formed an isolated cluster
407 in Ebino, in the far West of Miyazaki Prefecture, the sources inferred by Lau's modified model
408 agreed very closely with epidemiological field data whereas the sources for all four of these
409 premises inferred by SCOTTI were inferred to be over 60 km away. Whilst at least one of these
410 premises is likely to have been infected from the main focus of infection to the East, it is highly
411 unlikely that all four were infected in independent introductions. Considered together, the
412 inferences of Lau and SCOTTI's models provide a reasonably complete epidemiological and
413 phylogenetic inference for the Japanese outbreak.

414

415 **Conclusions**

416 Extending Lau's systematic Bayesian inference framework to incorporate additional parameters
417 representing predominant species and numbers of animals held on a farm resulted in improvements
418 in overall accuracy across a series of varied simulated outbreaks. Infected farms that held
419 predominantly pigs were estimated to have five times the transmissibility of infected cattle farms
420 and be 49% less susceptible. The farm-level incubation period was estimated to be 1 day shorter
421 than the latent period, suggesting a small window following onset of clinical signs to target
422 interventions may substantially reduce the risk of onwards transmission in future outbreaks.

423

424

425 **Acknowledgements**

426 This research was supported by an Australian Research Council Discovery Early Career Researcher
427 Award (project number DE160100477) and by the Japanese Ministry of Agriculture, Forestry and
428 Fisheries (Management Technologies for the Risk of Introduction of Livestock Infectious Diseases
429 and Their Wildlife-borne Spread in Japan, FY2018-2022). Components of this research were
430 undertaken on The University of Melbourne's High Performance Computing system SPARTAN [54].
431 The AADIS model was initially developed by the Australian Government Department of Agriculture
432 and Water Resources in collaboration with the University of New England and has kindly been made
433 available to support this research. The funders had no role in study design, data collection and
434 analysis, decision to publish or preparation of the manuscript. The authors would also like to
435 acknowledge helpful comments on the research provided by colleagues in the National Institute of
436 Animal Health, Japan and the Asia-Pacific Centre for Animal Health (University of Melbourne).

437

438 **Author contributions statement**

439 All authors were involved in design of the study. SF and YH conceived the modified model
440 formulation with input from ML and RB. SF wrote the main manuscript text and implemented all
441 analyses. All authors reviewed and commented on the manuscript.

442

443

444 References

- 445 1. Knight-Jones T, Rushton J. The economic impacts of foot and mouth disease—What are they,
446 how big are they and where do they occur? *Prev Vet Med.* 2013;112(3-4):161-73.
- 447 2. McLaws M, Ribble C. Description of recent foot and mouth disease outbreaks in nonendemic
448 areas: Exploring the relationship between early detection and epidemic size. *The Canadian*
449 *Veterinary Journal.* 2007;48(10):1051.
- 450 3. Cottam EM, Wadsworth J, Shaw AE, Rowlands RJ, Goatley L, Maan S, et al. Transmission
451 pathways of foot-and-mouth disease virus in the United Kingdom in 2007. *PLoS Pathog.*
452 2008;4(4):e1000050.
- 453 4. Lin Y-L, Jong M-H, Huang C-C, Shieh HK, Chang P-C. Genetic and antigenic characterization of
454 foot-and-mouth disease viruses isolated in Taiwan between 1998 and 2009. *Vet Microbiol.*
455 2010;145(1-2):34-40.
- 456 5. Muroga N, Hayama Y, Yamamoto T, Kurogi A, Tsuda T, Tsutsui T. The 2010 foot-and-mouth
457 disease epidemic in Japan. *J Vet Med Sci.* 2012;74(4):399-404.
- 458 6. Park J-H, Lee K-N, Ko Y-J, Kim S-M, Lee H-S, Shin Y-K, et al. Control of foot-and-mouth disease
459 during 2010–2011 epidemic, South Korea. *Emerging Infect Dis.* 2013;19(4):655.
- 460 7. Jamal SM, Belsham GJ. Foot-and-mouth disease: past, present and future. *Vet Res.*
461 2013;44(1):116.
- 462 8. Kao RR, Haydon DT, Lycett SJ, Murcia PR. Supersize me: how whole-genome sequencing and
463 big data are transforming epidemiology. *Trends Microbiol.* 2014;22(5):282-91.
- 464 9. Hall M, Woolhouse M, Rambaut A. Epidemic reconstruction in a phylogenetics framework:
465 transmission trees as partitions of the node set. *PLoS Comput Biol.* 2015;11(12):e1004613.
- 466 10. Klinkenberg D, Backer JA, Didelot X, Colijn C, Wallinga J. Simultaneous inference of
467 phylogenetic and transmission trees in infectious disease outbreaks. *PLoS Comput Biol.*
468 2017;13(5):e1005495.
- 469 11. Lau MS, Dalziel BD, Funk S, McClelland A, Tiffany A, Riley S, et al. Spatial and temporal
470 dynamics of superspreading events in the 2014–2015 West Africa Ebola epidemic. *Proceedings of*
471 *the National Academy of Sciences.* 2017;114(9):2337-42.
- 472 12. Lau MS, Marion G, Streftaris G, Gibson G. A systematic Bayesian integration of
473 epidemiological and genetic data. *PLoS Comput Biol.* 2015;11(11):e1004633.
- 474 13. Morelli MJ, Thébaud G, Chadœuf J, King DP, Haydon DT, Soubeyrand S. A bayesian inference
475 framework to reconstruct transmission trees using epidemiological and genetic data. *PLoS Comput*
476 *Biol.* 2012;8(11):e1002768.
- 477 14. De Maio N, Wu C-H, Wilson DJ. SCOTTI: Efficient Reconstruction of Transmission within
478 Outbreaks with the Structured Coalescent. *PLoS Comput Biol.* 2016;12(9):e1005130.
- 479 15. Firestone SM, Hayama Y, Bradhurst RA, Yamamoto T, Tsutsui T, Stevenson MA.
480 Reconstructing outbreaks: a methods comparison of transmission network models. *Sci Rep.* 2019.
- 481 16. Cottam EM, Thébaud G, Wadsworth J, Gloster J, Mansley L, Paton DJ, et al. Integrating
482 genetic and epidemiological data to determine transmission pathways of foot-and-mouth disease
483 virus. *Proc R Soc Lond B Biol Sci.* 2008;275(1637):887-95.
- 484 17. Nishiura H, Omori R. An Epidemiological Analysis of the Foot-and-Mouth Disease Epidemic in
485 Miyazaki, Japan, 2010. *Transbound Emerg Dis.* 2010;57(6):396-403.
- 486 18. Hayama Y, Muroga N, Nishida T, Kobayashi S, Tsutsui T. Risk factors for local spread of foot-
487 and-mouth disease, 2010 epidemic in Japan. *Res Vet Sci.* 2012;93(2):631-5.
- 488 19. Muroga N, Kobayashi S, Nishida T, Hayama Y, Kawano T, Yamamoto T, et al. Risk factors for
489 the transmission of foot-and-mouth disease during the 2010 outbreak in Japan: a case–control
490 study. *BMC Vet Res.* 2013;9(1):150.
- 491 20. Nishi T, Yamada M, Fukai K, Shimada N, Morioka K, Yoshida K, et al. Genome variability of
492 foot-and-mouth disease virus during the short period of the 2010 epidemic in Japan. *Vet Microbiol.*
493 2017;199:62-7.

- 494 21. Wada M, Stevenson M, Cogger N, Carpenter T. Evaluation of the Control Strategy for the
495 2010 Foot-and-Mouth Disease Outbreak in Japan Using Disease Simulation. *Transbound Emerg Dis.*
496 2016. doi: 10.1111/tbed.12467. PubMed PMID: 26748445.
- 497 22. Akashi H. The 2010 Foot-and-Mouth Disease Outbreak in Miyazaki Prefecture. *Journal of*
498 *Disaster Research.* 2012;7(3):252-7.
- 499 23. Hayama Y, Yamamoto T, Kobayashi S, Muroga N, Tsutsui T. Mathematical model of the 2010
500 foot-and-mouth disease epidemic in Japan and evaluation of control measures. *Prev Vet Med.*
501 2013;112(3-4):183-93.
- 502 24. Tildesley MJ, Deardon R, Savill NJ, Bessell PR, Brooks SP, Woolhouse MEJ, et al. Accuracy of
503 models for the 2001 foot-and-mouth epidemic. *Proc R Soc Lond B Biol Sci.* 2008;275(1641):1459-68.
504 doi: 10.1098/rspb.2008.0006. PubMed PMID: ISI:000255503300014.
- 505 25. Alexandersen S, Zhang Z, Donaldson A, Garland A. The pathogenesis and diagnosis of foot-
506 and-mouth disease. *J Comp Pathol.* 2003;129(1):1-36.
- 507 26. Keeling MJ, Woolhouse MEJ, Shaw DJ, Matthews L, Chase-Topping M, Haydon DT, et al.
508 Dynamics of the 2001 UK foot and mouth epidemic: stochastic dispersal in a heterogeneous
509 landscape. *Sci.* 2001;294(5543):813-7. PubMed PMID: ISI:000171851800036.
- 510 27. Lau MS. Novel Bayesian inference in epidemics – model assessment and integrating
511 epidemiological and genetic data: Heriot-Watt University; 2015.
- 512 28. Sellke T. On the asymptotic distribution of the size of a stochastic epidemic. *Journal of*
513 *Applied Probability.* 1983;20(2):390-4.
- 514 29. Bradhurst RA, Roche SE, East IJ, Kwan P, Garner MG. A hybrid modeling approach to
515 simulating foot-and-mouth disease outbreaks in Australian livestock. *Frontiers in Environmental*
516 *Science.* 2015;3:17.
- 517 30. Rambaut A, Grass NC. Seq-Gen: an application for the Monte Carlo simulation of DNA
518 sequence evolution along phylogenetic trees. *Bioinformatics.* 1997;13(3):235-8.
- 519 31. Martin DP, Murrell B, Golden M, Khoosal A, Muhire B. RDP4: Detection and analysis of
520 recombination patterns in virus genomes. *Virus evolution.* 2015;1(1).
- 521 32. Kumar S, Stecher G, Tamura K. MEGA7: molecular evolutionary genetics analysis version 7.0
522 for bigger datasets. *Mol Biol Evol.* 2016;33(7):1870-4.
- 523 33. Gelman A, Rubin DB. Inference from iterative simulation using multiple sequences. *Statistical*
524 *science.* 1992;457-72.
- 525 34. Rambaut A, Drummond AJ, Xie D, Baele G, Suchard MA. Posterior summarisation in Bayesian
526 phylogenetics using Tracer 1.7. *Syst Biol.* 2018;10.
- 527 35. Bouckaert R, Heled J, Kühnert D, Vaughan T, Wu C-H, Xie D, et al. BEAST 2: a software
528 platform for Bayesian evolutionary analysis. *PLoS Comput Biol.* 2014;10(4):e1003537.
- 529 36. Hasegawa M, Kishino H, Yano T-a. Dating of the human-ape splitting by a molecular clock of
530 mitochondrial DNA. *J Mol Evol.* 1985;22(2):160-74.
- 531 37. Firestone SM, Lau MSY, Kodikara S, Demirhan H, Hayama Y, Yamamoto T, et al. Bayesian
532 Outbreak Reconstruction Inference and Simulation (BORIS). GitHub repository,
533 <https://github.com/sfires/BORIS>, accessed 24/6/2019); 2019.
- 534 38. R Core Team. R: A language and environment for statistical computing. R Foundation for
535 Statistical Computing, Vienna, Austria.: <http://www.R-project.org/>, accessed 24/6/2019); 2019.
- 536 39. Stevenson M, Nunes T, Heuer C, Marshall J, Sanchez J, Thornton R, et al. epiR: Tools for the
537 Analysis of Epidemiological Data. R package version 0.9-96. 2018.
- 538 40. Handcock MS, Hunter DR, Butts CT, Goodreau SM, Morris M. statnet: Software Tools for the
539 Representation, Visualization, Analysis and Simulation of Network Data. *Journal of Statistical*
540 *Software.* 2008;24(1):1-11.
- 541 41. Plummer M, Best N, Cowles K, Vines K. CODA: Convergence Diagnosis and Output Analysis
542 for MCMC. *R News.* 2006;6:7-11.
- 543 42. Wickham H. ggplot2: elegant graphics for data analysis: Springer; 2016.

- 544 43. Pfeiffer CN, Campbell AJD, Firestone SM, Larsen JWA, Stevenson MA. Sample size
545 considerations for livestock movement network data. *Prev Vet Med.* 2015;122:399–405.
- 546 44. Hayama Y, Firestone SM, Stevenson MA, Yamamoto T, Shimizu Y, Tsutsui T. Reconstructing a
547 transmission network and identifying risk factors of secondary transmissions in the 2010 FMD
548 outbreak in Japan. *Transbound Emerg Dis.* 2019.
- 549 45. Mardones F, Perez A, Sanchez J, Alkhamis M, Carpenter T. Parameterization of the duration
550 of infection stages of serotype O foot-and-mouth disease virus: an analytical review and meta-
551 analysis with application to simulation models. *Vet Res.* 2010;41(4):45.
- 552 46. Charleston B, Bankowski BM, Gubbins S, Chase-Topping ME, Schley D, Howey R, et al.
553 Relationship between clinical signs and transmission of an infectious disease and the implications for
554 control. *Sci.* 2011;332(6030):726-9.
- 555 47. Sellers R, Parker J. Airborne excretion of foot-and-mouth disease virus. *Epidemiol Infect.*
556 1969;67(4):671-7.
- 557 48. Fukai K, Morioka K, Yoshida K. An experimental infection in pigs using a foot-and-mouth
558 disease virus isolated from the 2010 epidemic in Japan. *J Vet Med Sci.* 2011;73(9):1207-10.
- 559 49. Onozato H, Fukai K, Kitano R, Yamazoe R, Morioka K, Yamada M, et al. Experimental
560 infection of cattle and goats with a foot-and-mouth disease virus isolate from the 2010 epidemic in
561 Japan. *Arch Virol.* 2014;159(11):2901-8.
- 562 50. Browning G, Caswell J, Cobb S, Fox L, French N, Humphris M, et al. Technical Advisory Group
563 report to Ministry of Primary Industries New Zealand: TAG response 17 May 2018: Feasibility of
564 eradication of *Mycoplasma bovis*. 2018.
- 565 51. Jewell CP, Keeling MJ, Roberts GO. Predicting undetected infections during the 2007 foot-
566 and-mouth disease outbreak. *J R Soc Interface.* 2009;6(41):1145-51. doi: 10.1098/rsif.2008.0433.
567 PubMed PMID: ISI:000271464500004.
- 568 52. Jombart T, Cori A, Didelot X, Cauchemez S, Fraser C, Ferguson N. Bayesian reconstruction of
569 disease outbreaks by combining epidemiologic and genomic data. *PLoS Comput Biol.*
570 2014;10(1):e1003457.
- 571 53. Drummond AJ, Suchard MA, Xie D, Rambaut A. Bayesian phylogenetics with BEAUti and the
572 BEAST 1.7. *Mol Biol Evol.* 2012;29(8):1969-73.
- 573 54. Lafayette L, Sauter G, Vu L, Meade B. Spartan Performance and Flexibility: An HPC-Cloud
574 Chimera, OpenStack Summit, Barcelona2016.

575

576

577 **Table 1: Key parameters in the Bayesian MCMC inference.**

Parameter	Type	Description
$t.samp_j, S_j$	Observed	The timing of sampling and available sequences for infected premises in the dataset.
ψ_j, t_{e_j}, t_{i_j}	Latent	The source and timing of exposure and onset of infectiousness for each exposed site j .
Gt_j	Latent	The sequence on each infected premises at each sampling and transmission time (t).
α	Latent	The background rate of infection.
β, β_{ij}	Latent	The secondary transmission rate, with and without additional farm-level covariates.
d_{ij}	Observed	Euclidean distance between premises i and j .
κ	Latent	The power of the spatial transmission kernel.
n_i, n_j	Observed	Number of animals on premises i and j .
ν	Latent	The effect (power) of number of animals on premises-level infectivity for farms.
τ	Latent	The effect (power) of number of animals on premises-level susceptibility for farms.
$\phi_{cattle}, \phi_{pig}, \phi_{other}$	Latent	The multiplicative effect of predominant species on premises-level infectivity.
ρ_{pig}, ρ_{other}	Latent	The multiplicative effect of predominant species on premises-level susceptibility.
μ_1, μ_2	Latent	The rates of transitions and transversions.
$mean(lat), var(lat)$	Latent	The mean and variance of the duration of the farm-level latent period.
c	Latent	The mean period from onset of infectiousness to the last day of culling (i.e., the farm-level infectious period).
p	Latent	Probability that a nucleotide base of a primary sequences differs from that in the universal master sequence.

578

579 **Table 2: Epidemiological and phylogenetic parameters inferred for the 2010 outbreak of foot-and-mouth disease in Miyazaki Prefecture, Japan, by**
580 **transmission network model.**

Model parameter (units)	Lau's joint inference, modified Posterior Median [95% HPD]	Structured Coalescent Transmission Tree Inference Posterior Median [95% HPD]
Primary transmission rate, α	4.0×10^{-5} [0.1×10^{-5} , 2.1×10^{-4}]	—
Secondary transmission rate, β	0.063 [0.016, 0.142]	—
Mutation rate (substitutions site ⁻¹ day ⁻¹)	1.83×10^{-5} [1.63×10^{-5} , 2.06×10^{-5}]	2.31×10^{-5} [1.73×10^{-5} , 2.89×10^{-5}]
Transition to transversion ratio	6.95 [5.20, 9.57]	10.12 [6.68, 14.33]
Delay from origin of epidemic to outbreak detection (days)	30.9 [25.9, 42.3]	38.5 [24.4, 56.5]
Effective population size ^a	—	18.9 [8.6, 34.5]
Number of farms infected at outbreak detection	15 [11, 30]	—
Farm-level incubation period (days)	5.6 [2.6, 13.8]	—
Farm-level latent period, <i>mean(lat)</i> (days)	6.8 [5.2, 8.1]	—
Farm-level infectious period, <i>c</i> (days)	15.2 [13.6, 17.2]	—
Spatial kernel scaling parameter, κ	1.79 [1.54, 2.04]	—
Infectivity of pig farms vs. cattle farms, ϕ_{pigs}	5.15 [2.64, 11.59]	—
Infectivity of other farms vs. cattle farms, ϕ_{other}	0.50 [0.11, 1.67]	—
Effect of farm size on infectivity, ν	0.08 [0.00, 0.26]	—
Susceptibility of pig farms vs. cattle farms, ρ_{pigs}	0.51 [0.30, 0.83]	—
Susceptibility of other farms vs. cattle farms, ρ_{other}	0.45 [0.14, 1.22]	—
Effect of farm size on susceptibility, τ	0.23 [0.11, 0.35]	—

581 HPD = Highest probability density region; IP = infected premises. ^a Estimated from structured coalescent migratory model based on within-host (here, within-farm) effective
582 population size (N_e), migration rate and proportion of hosts with consensus support that their source was sampled.

583 **Figure legends**

584

585 **Figure 1: Comparison of the accuracy of inferences of proposed sources of infection for six**
586 **simulated outbreaks of foot-and-mouth disease in Japan and Australia.** Black line = original
587 formulation; red = modified model. Runs J1, J2 and J3 simulated in the same framework as the
588 modified model. Runs A1, A2, A3 simulated in using the Australian Animal Disease Simulation model.
589 Accuracy was defined as the proportion of infected premises for which the true source was the
590 proposed source with the highest posterior probability density. Vertical reference lines denote
591 proposed ancestors with >50% and >80% model support, respectively.

592

593 **Figure 2: Inferred transmission network for the 2010 outbreak of foot-and-mouth disease in**
594 **Miyazaki Prefecture, Japan, in arbitrary space.** Model support for the proposed ancestor
595 represented by edge width. Darker shading of edges represents earlier inferred transmission events
596 in the outbreak. Farms holding predominantly pigs, cattle and other species are represented by pink,
597 white and blue nodes, respectively. Case numbers randomised for confidentiality.

598

599 **Figure 3: Inferred spatial transmission kernel shape for the 2010 outbreak of foot-and-mouth**
600 **disease in Miyazaki Prefecture, Japan.** Bold line represents posterior median prediction and dashed
601 lines represent 95% highest probability density region.

602

603 **Figure 4: Estimated transmission windows based on Cottam's frequentist approach for the first 20**
604 **infected premises detected for which genomic data were available in the 2010 outbreak of foot-**
605 **and-mouth disease in Miyazaki Prefecture, Japan.** Black lines represent most likely period of the
606 earliest infection of an animal on each infected premises (IP), grey lines represent estimated
607 duration of infectiousness at the premises level, tapering as culling commences. The red reference
608 line represents the point of outbreak detection on 20 April 2010. On the most likely day that Farm B
609 was infected, only Farm A was possibly infectious.

610

611 **Supplementary Materials**

612

613 **S1: Simulated outbreak datasets: data and parameterisation.**

614

615 **S2: Comparison of the accuracy of the original model and modifications of Lau's joint Bayesian**
616 **transmission network inference for inferring sources for simulated outbreaks of foot-and-mouth**
617 **disease in Japan and Australia.**

618

619 **S3: Comparison of the accuracy of the original model and modifications of Lau's joint Bayesian**
620 **transmission network inference for inferring epidemiological and phylogenetic parameters for**
621 **simulated outbreaks of foot-and-mouth disease in Japan and Australia.** Model formulations
622 abbreviated as follows: orig = original; mod = modified; mod-n = modified-normalised.

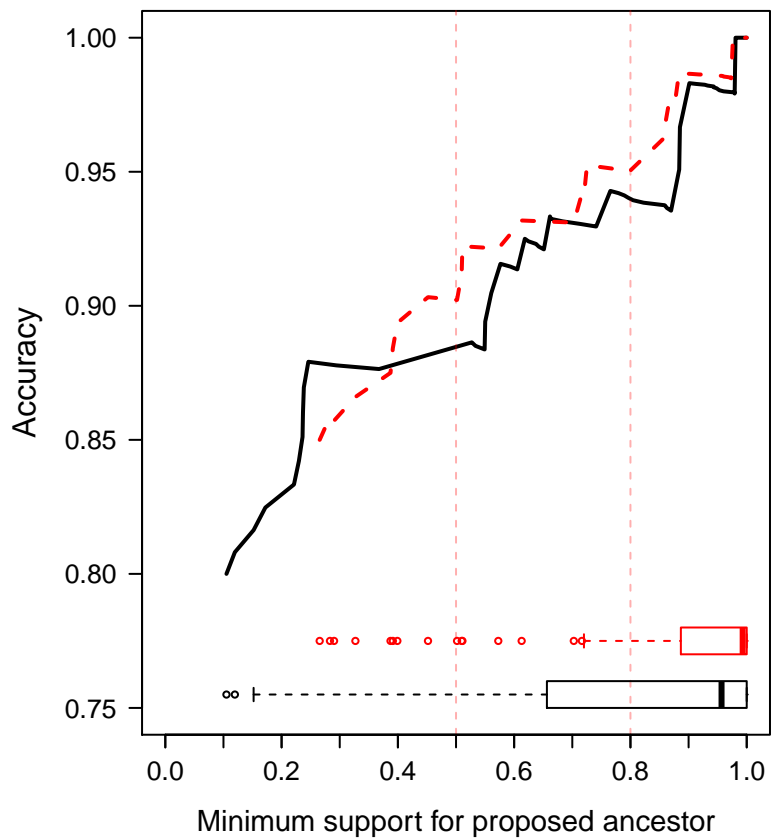
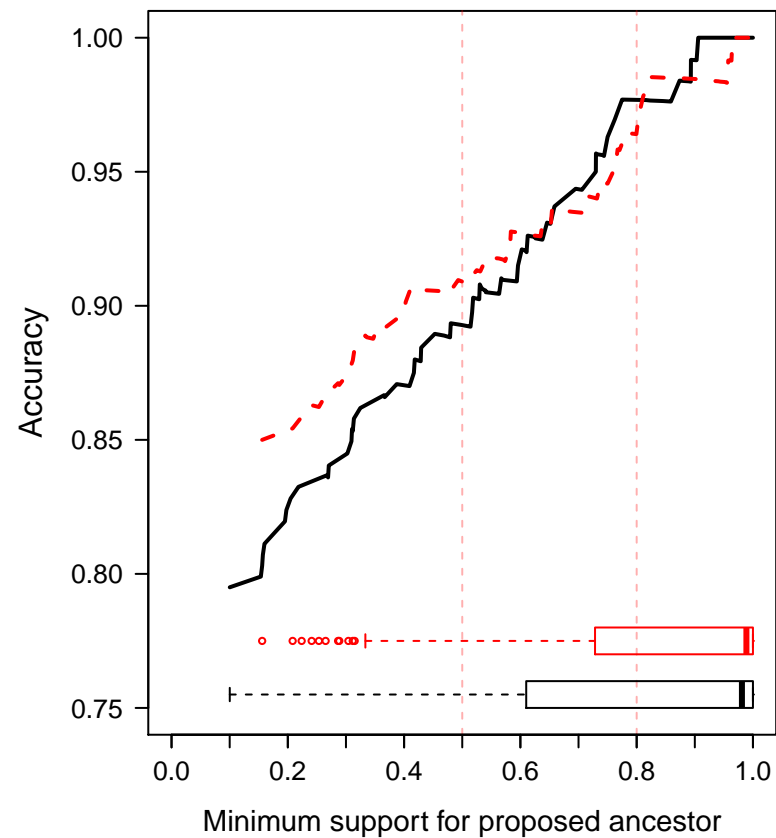
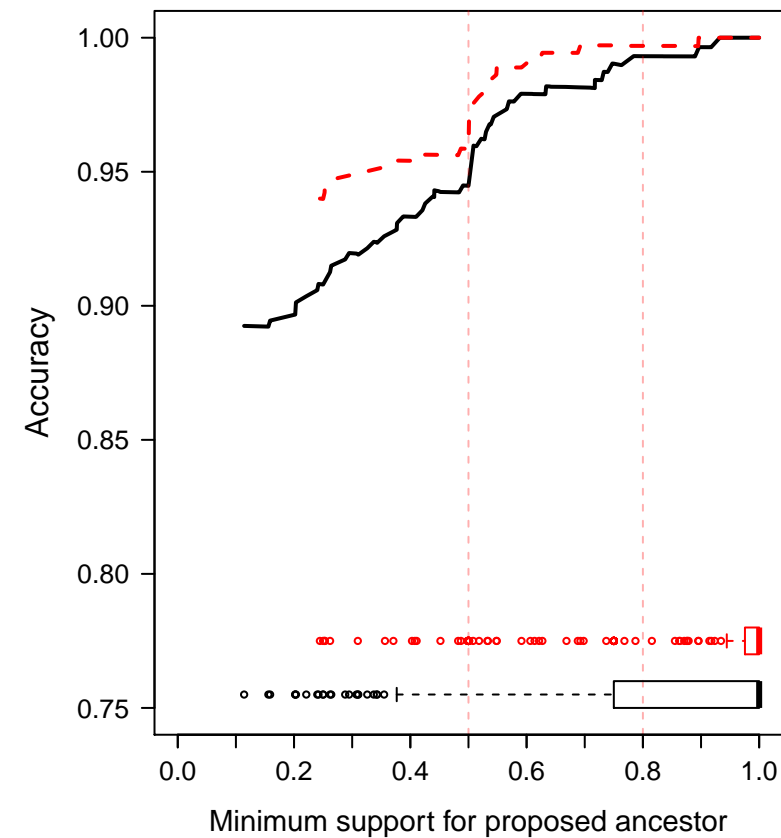
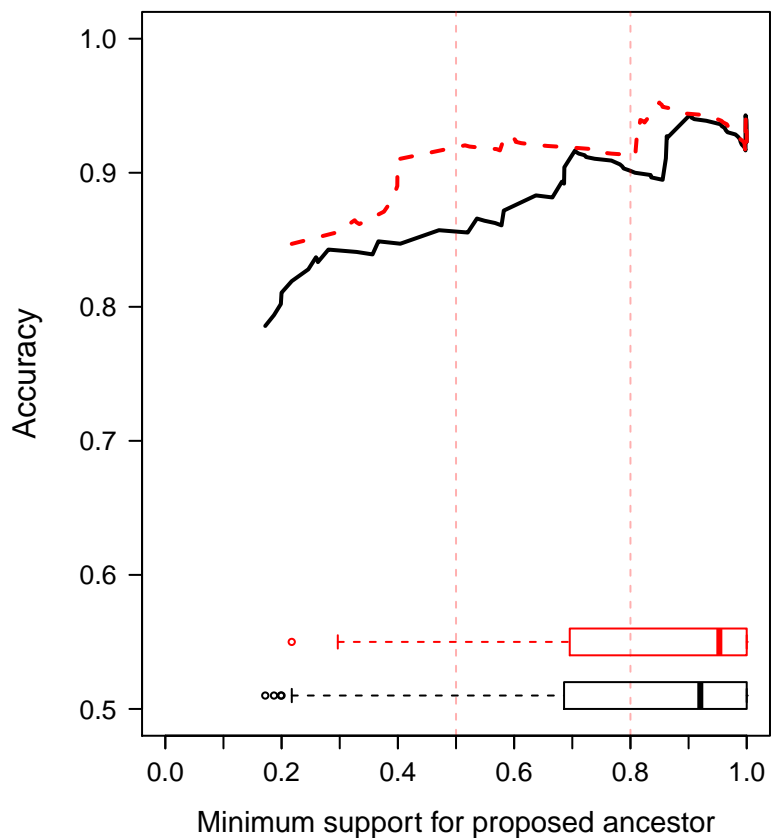
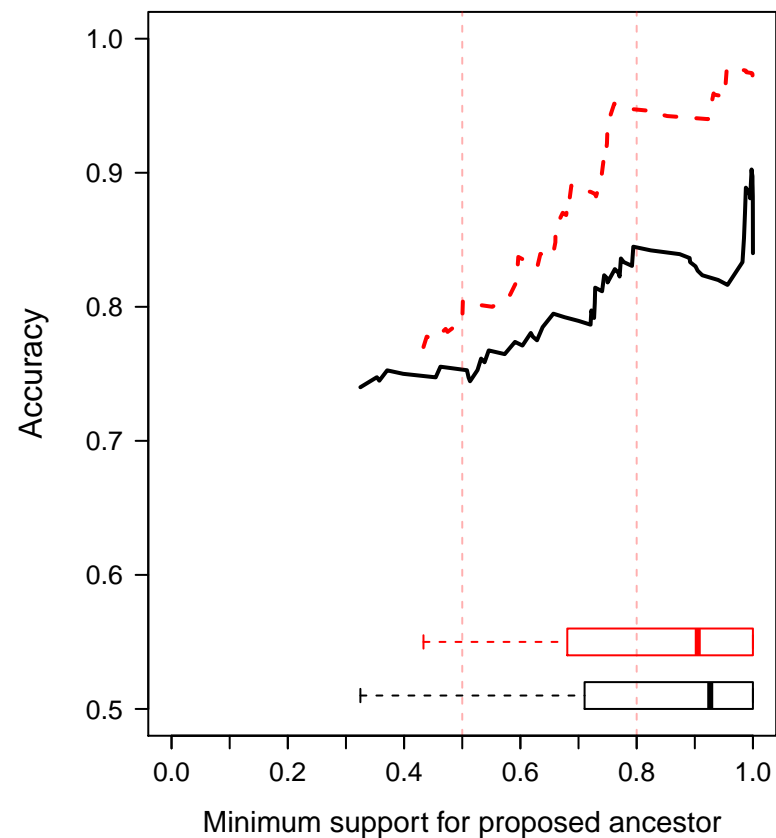
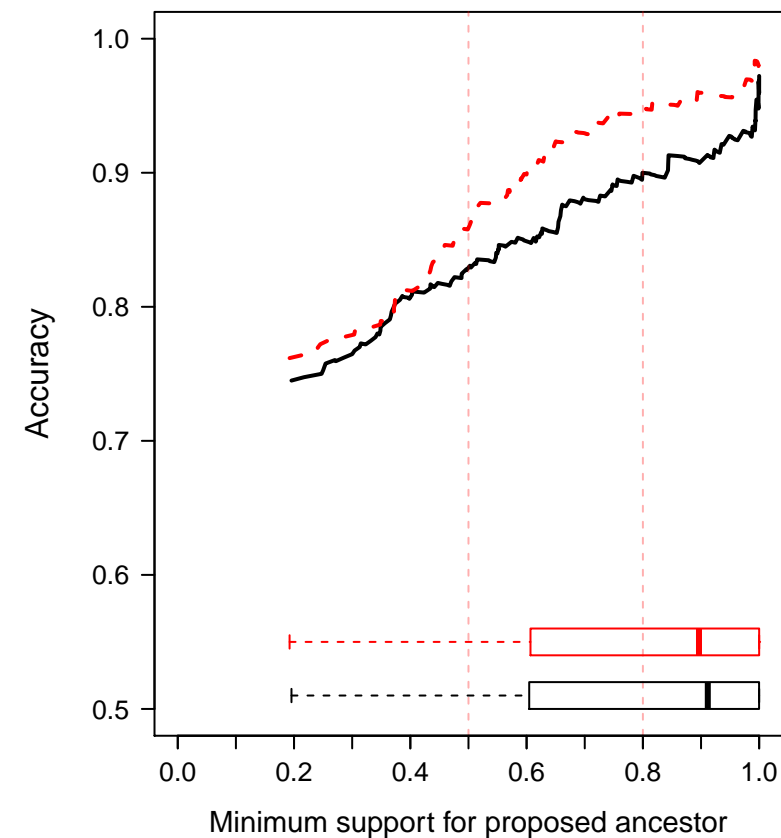
623

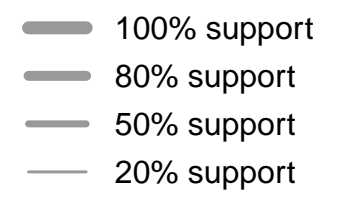
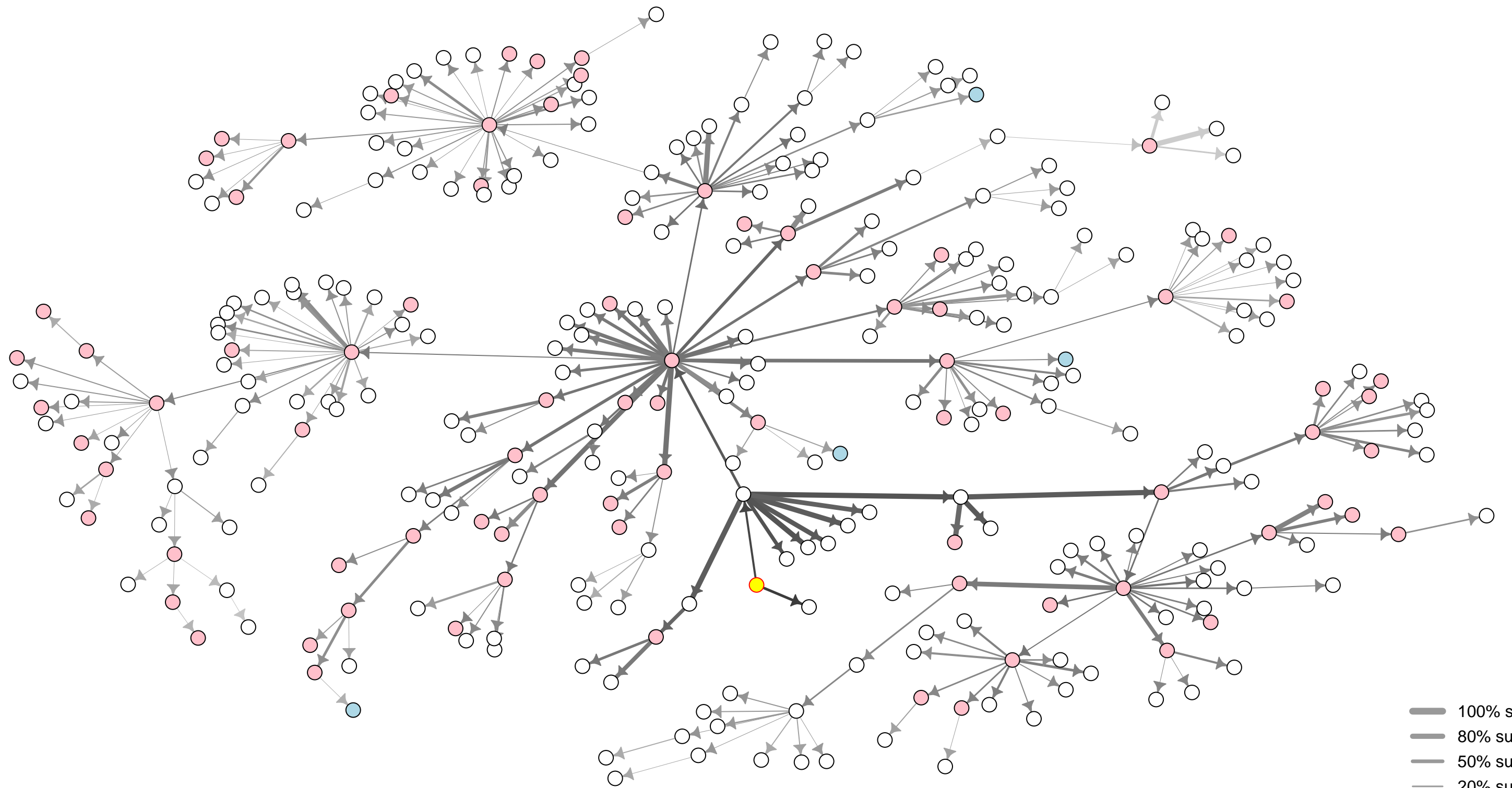
624 **S4: Nucleotide substitution model fit for genomic data from the 2010 outbreak of foot-and-mouth**
625 **disease in Japan.**

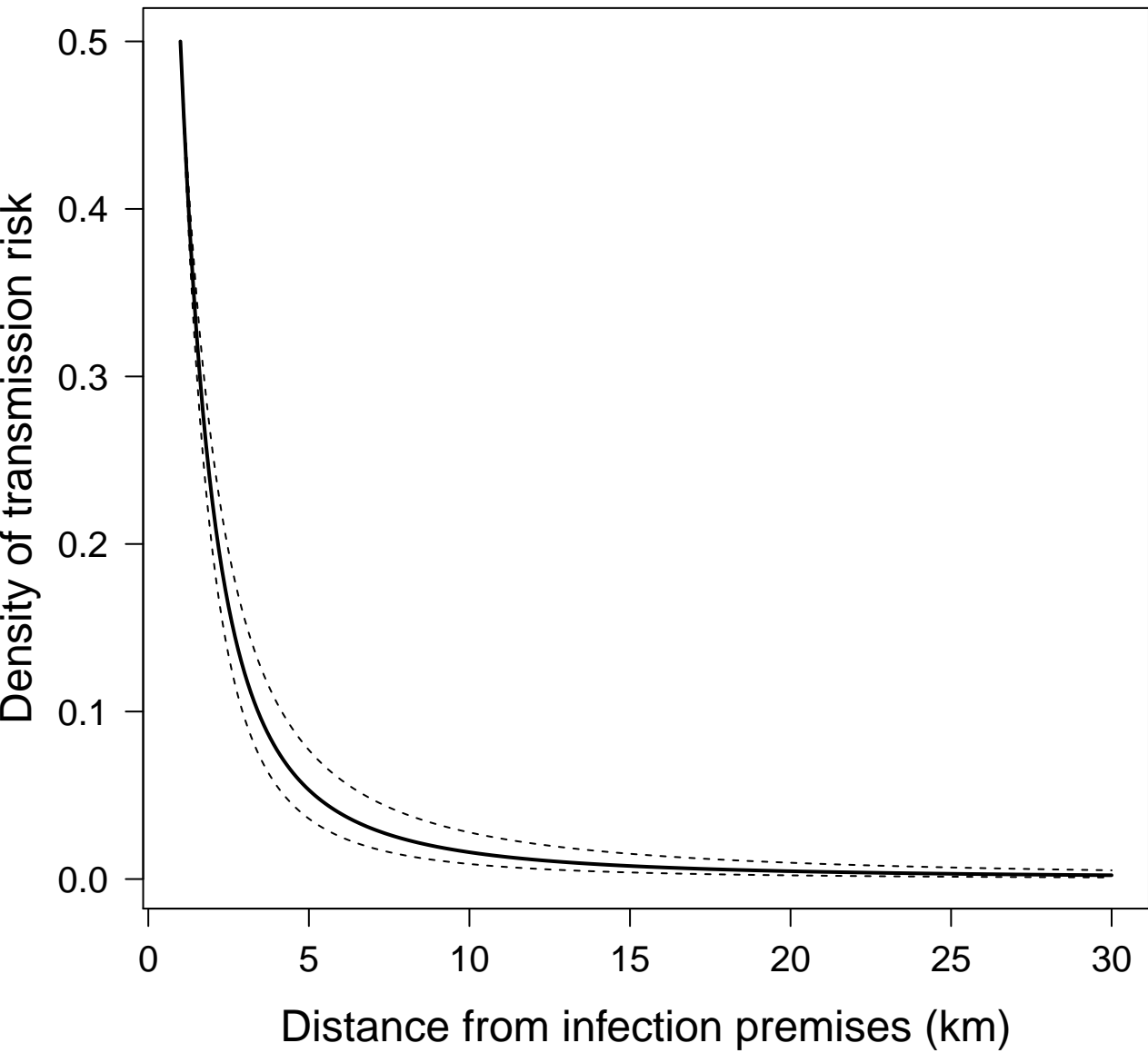
626

627 **S5: Lau model (original and modified-normalised) inferred transmission networks and estimates**
628 **for the 2010 outbreak of foot-and-mouth disease in Miyazaki Prefecture, Japan.**

629

Run: J1**Run: J2****Run: J3****Run: A1****Run: A2****Run: A3**





Temporal risk windows

Farm ID

